ChemComm

Accepted Manuscript

ROYAL SOCIETY OF CHEMISTRY

rsc.li/chemcomm

ChemComm

View Article Online
DOI: 10.1039/C8CC05369C

COMMUNICATION

A covalent organic framework bearing thioether pendant arms for selective detection and recovery of Au from ultra-low concentration aqueous solution

Received 10th July 2018,
Accepted 30th July 2018

DOI: 10.1039/x0xx00000x

www.rsc.org/

Zhiming Zhou,[ab] Wanfu Zhong,[ab] Kaixun Cui,[ab] Zanyong Zhuang,[ab] Lingyun Li,[ab] Liuyi Li,*[ab] Jinhong Bi[b] and Yan Yu*[ab]

A fluorescent covalent organic framework (COF), featuring precise distribution of thioether pendant arms inside the cavity, was designed. The thioether-functionalized COF exhibits selective sensing and capture of Au ions at ultra-trace levels in water with high sensitivity, selectivity and adsorption capacity, which makes it an excellent candidate for selective detection and recovery of Au.

The recovery of Au from electronic wastes is extremely both important from environmental and economic point of views, because of its limited availability and high price. Much effort has been devoted to develop alternative methods to the highly toxic cyanide heap leaching process[1] to recovery of Au from high-concentration solution.[2] However, little work has been done on selective detection and separation of Au from ultra-low concentration aqueous solution, as it requires sensitive response and specific affinity to Au.

Covalent organic frameworks (COFs) are one of new crystalline porous materials with well-defined structures.[3] The structure tunability and permanent porosity make COFs a promising materials platform for functional design.[4] Furthermore, the extended π-conjugation in COFs endows them with fluorescent property,[5] endowing them emerging candidates for sensing applications.[6] We envision that introduction of Au-binding sites inside the cavity of fluorescent COFs may endow them with an ability to selectively detect and recover low concentration Au. Such COFs would have specific affinity of the binding sites in COFs to Au ions, providing a great potential for selective adsorption of low concentration Au from water.[7] Another possible advantage of such a COF-based recovery system is that through the establishment of a relationship between the metal ions and luminescence characteristics of the COFs,[6d] selective sensing of Au ions may be achieved.

Herein, we report a design of thioether-functionalized COF (TTB-COF) for selective sensing and recovery of low concentration Au in water (Scheme 1). TTB-COF exhibits the function of selectively, qualitatively, and quantitatively recognizing Au over other metal ions at low concentration levels by significant luminescence quenching through the strong and selective affinity of sulfur atoms for Au ions.

TTB-COF bearing thioether pendant arms as binding sites for Au[8] was solvothermally synthesized through the reversible imine condensation reaction of 2,5-bis(2-(ethylthio)ethoxy) terephthalohydrazide (BETH) and 1,3,5-triformylbenzene (TFB). Fourier transform infrared spectroscopy (FT-IR) spectrum of TTB-COF (Fig. S1, ESI†) showed a new characteristic vibrational band appeared at 1620 cm^{-1},[9] revealing the formation of the imine bonds via the successful condensation of BETH and TFB. Solid-state ^{13}C NMR spectroscopy further supports the proposed chemical structures of TTB-COF. The formation of the imine bond was established by a characteristic resonance signal

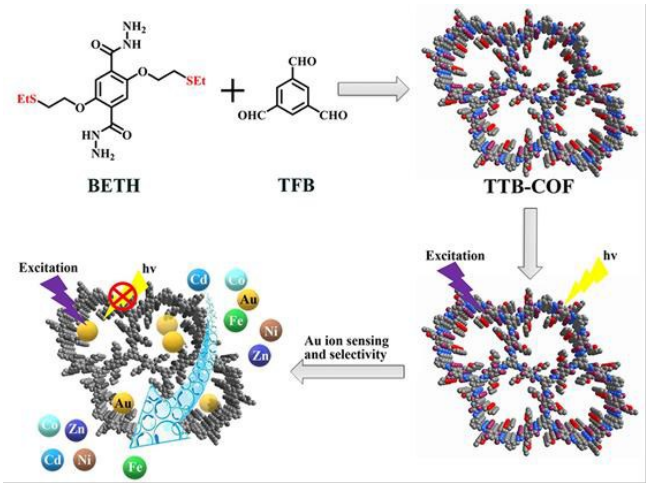

Scheme 1 Schematic representation of the synthesis of TTB-COF and its application in selective detection and capture of Au ions.

[a] College of Materials Science and Engineering, Fuzhou University, Minhou,Fujian 350108, China. E-mail address: lyli@fzu.edu.cn; yuyan@fzu.edu.cn
[b] Key Laboratory of Eco-materials Advanced Technology (Fuzhou University), Fuzhou, Fujian 350108, China.
†Electronic Supplementary Information (ESI) available. See DOI: 10.1039/x0xx00000x

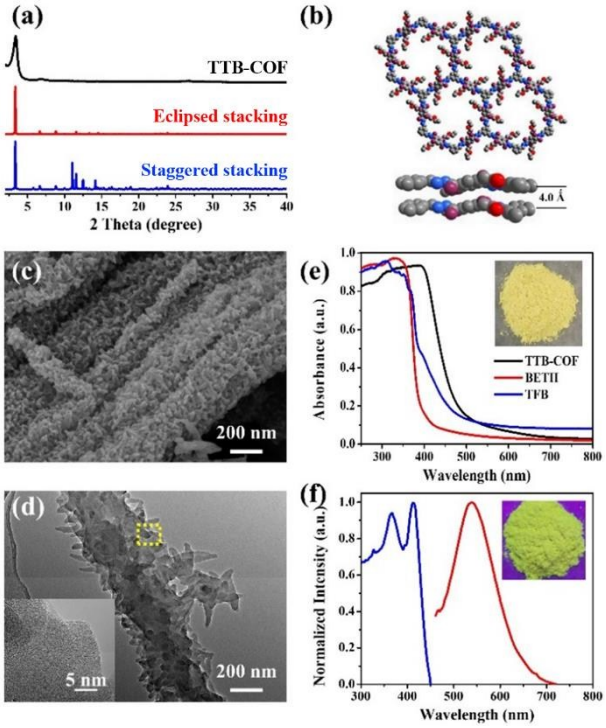

Fig. 1 (a) XRD patterns of experimental and simulated TTB-COF; (b) Top and side views of the eclipsed structure of TTB-COF (red, S; blue, N; gray, C; purple, O); (c) SEM and (d) TEM images of TTB-COF; (e) UV-vis absorption spectra of TTB-COF, BETH, and TFB. Inset: photos of TTB-COF; (f) Fluorescence excitation (blue line) and emission (red line) spectra of TTB-COF in solid state. Inset: TTB-COF under UV-light (365 nm).

at 160 ppm,[10] while the signals at 15 and 36 ppm confirmed the presence of thioether groups in the framework (Fig. S2, ESI†).[11] Elemental analyses of the content of C, H, N and S in TTB-COF were in good agreement with the theoretical values. In addition, the TTB-COF could be synthesized conveniently in various solvent systems (Fig. S3 and S4, ESI†), showing its facile synthesis. TTB-COF was insoluble and stable in common organic solvents and water (Fig. S5, ESI†), in particular, it can resist acid, even in aqueous 1M HCl at 100 °C for 24 h (Fig. S6, ESI†). Thermogravimetric analysis (TGA) shows that TTB-COF is stable to 280 °C (Fig. S7, ESI†). Such chemical and thermal stability makes TTB-COF attractive for use in metal ions recovery from water.

The crystallinity of TTB-COF is determined by powder X-ray diffraction (XRD) analyses. A set of intensive peaks at 2θ = 3.2°, 7.3°, and 25.7° were observed in the experimental XRD pattern (Fig. 1a and Fig. S8), which are assignable to 100, 200, and 001 facets, respectively. To determine the packing manner of TTB-COF, theoretical simulations are carried out using Materials Studio software packages. The eclipsed stacking model (Fig. 1b) is in remarkable agreement with the experimental XRD pattern in terms of peak positions and relative intensities (Fig. 1a), suggesting the 2D layers adopt eclipsed packing. By contrast, the calculated XRD pattern for the staggered structure cannot be consistent with the experimental XRD patterns (Fig. S9, ESI†).

The porosity of TTB-COF is studied by measuring N_2 adsorption at 77 K. The BET surface area and pore volume are 36 $m^2 g^{-1}$ and 0.06 $cm^3 g^{-1}$, respectively (Fig. S10, ESI†). The relatively lower surface area than that of the theoretical value (2929 $m^2 g^{-1}$) was mainly owing to the blockage of the surface pore channels by small COF nanoparticles. The pore size distribution reveals a homogeneous pore diameter of 1.4 nm (Fig. S10, Inset, ESI†), which is consistent with the pore size predicted from the crystal structures (1.7 nm). Scanning electron microscopy (SEM) images show TTB-COF consists of uniform microrods with a size of about 200 nm in diameter (Fig. 1c). The microrods are consisted from the primary nanosheets with a few nanometers in thickness (Fig. S11, ESI†). The sheaf-like TTB-COF hierarchical microrods were clearly observed by TEM spectra (Fig. 1d and Fig. S12, ESI†). From the enlarged image of one microrod, the microrod was constructed by many interconnected nanosheets. Such a hierarchical structure is would be beneficial for rapid mass transfer.[12]

UV-visible diffuse-reflectance spectrum (UV-Vis DRS) of TTB-COF shows a broad absorption up to 700 nm in the solid state (Fig. 1e). A maximum absorption at 400-550 nm is assigned to the π–π* transitions of the conjugated ring systems. A large bathochromic shift of TTB-COF from that of monomers is attributed to the extended π-conjugation in TTB-COF. TTB-COF is yellow in color (Inset in Fig. 1e), while it displays a bright yellow photoluminescence when excited under 365 UV-light (Inset in Fig. 1f). Upon excitation at 394 nm, TTB-COF in solid state exhibits a maximum emission band at 540 nm with an absolute quantum yield (Φ_F) of 4.2% (Fig. 1f). Under the same excitation wavelength, the monomers BETH and TFB display weak fluorescence emission peaks at 513 and 470 nm, respectively (Fig. S13, ESI†). The strong fluorescence in TTB-COF was mainly attributed to the existence of a p-n heterojunction between BETH and TFB units[6b] as well as the contorted structure.[6a, 6d] It is worth mentioning that TTB-COF keeps its high fluorescence in H_2O, ethanol, acetonitrile, THF and DMF (excitation wavelength λ_{ex}= 394 nm, Fig. S14, ESI†), which is the prerequisite for its potential application as fluorescent sensing probes in solution.

Density functional theory (DFT) calculations (B3LYP/6-311g**) of the optimized structure of building block shows that the pendant thioether groups is electronically negative (Fig. S15, ESI†), demonstrating that the thioether groups should preferably coordinate to metal ions. The lowest unoccupied molecular orbitals (LUMOs) and highest occupied molecular orbitals (HOMOs) of the building block are similarly delocalized over the entire conjugated structure and the band gap is estimated to be 3.90 eV (Fig. S16, ESI†).

TTB-COF with fluorescent properties and the specific affinity of pendant sulfur groups as well as the open pore structure can be exploited as an ideal candidate for sensing and adsorption of Au ions. As shown in Fig. 2a, the fluorescence intensity of TTB-COF gradually decreased with increasing Au ions concentration, accompanied by its color change under a UV lamp (with λ_{ex} = 365 nm) (Inset in Fig. 2a). The fluorescence intensity at 540 nm of TTB-COF was significantly quenched with the addition of 0.83 μM of Au ions. 84% of the total fluorescence intensity of TTB-COF was quenched with the addition of 10 μM of Au ions. The comparison of the UV-vis spectrum of Au ions, fluorescence excitation and emission spectra of TTB-COF demonstrates that

View Article Online
DOI: 10.1039/C8CC05369C

the used excitation wavelength (λ_{ex}=394 nm) does not overlap with the absorbance of Au ions (Fig. S17, ESI†), excluding the inner filter effect between Au ions and fluorescent TTB-COF. The plot of fluorescence intensity versus different concentration of Au ions showed a linear relationship in the range of 1.0-10.0 μM (Fig. 2b). The quenching constant (K_{sv}) is 4.46×10^5 M^{-1} from the linear Sterm-Volmer curve. The detection limit is calculated to be 0.87 μM based on S/N = 3. The high quenching rate constant (2.84×10^{14} M^{-1} s^{-1}) based on the K_{sv} and the fluorescence lifetime of TTB-COF (1.57 ns) (Fig. S18, ESI†) indicates that the quenching efficiency is mainly ascribed to the static quenching effect. The maximum capture capacity of TTB-COF is 560 mg g^{-1} (Fig. 2c). Even though the recovery experiments are carried out toward the low concentration Au, the sorption capacity is comparable with or higher than those of the most efficient materials reported earlier (Table S1, ESI†).[13] Moreover, the sensing of Au ions with TTB-COF can be carried out in water, and the detection limit is 1.39 μM (Fig. S19, ESI†), suggesting its high potential for practical applications. The adsorption kinetics of TTB-COF toward Au ions in water showed that over 98% of Au ions can be captured within 1 min (Fig. 2d).

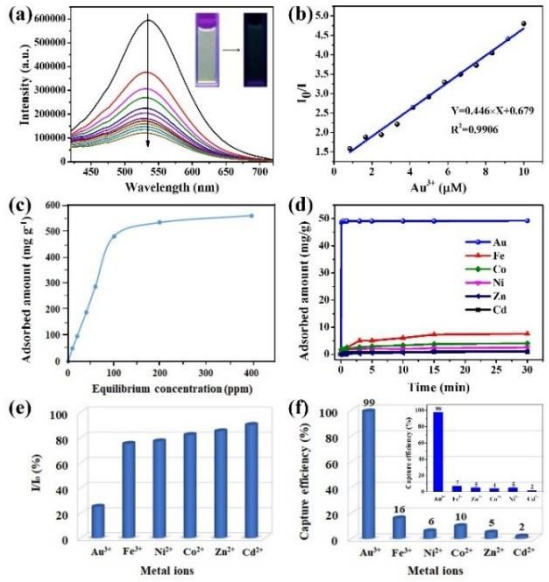

Fig. 2 (a) Fluorescence titration of TTB-COF in acetonitrile upon the gradual addition of Au ions (λ_{ex} = 394 nm), Inset: fluorescence images of quenching change of TTB-COF in acetonitrile upon the addition of Au ions (under a UV lamp with λ_{ex} = 365 nm); (b) Stern-Volmer plots for the quenching of TTB-COF by Au ions; (c) Au ions adsorption isotherm after 12 h; (d) Adsorption curves of various metal ions in aqueous solution. (e) Fluorescence response of TTB-COF in the presence of different metal ions in H_2O (λ_{ex} = 394 nm); (f) Capture efficiency for various metal ions. Inset: Capture efficiency of TTB-COF for Au ions in presence of other competing metal ions after adsorption for 90 minutes.

Selectivity is an important factor for practical Au sensing and recovery from water. As shown in Fig. 2e, Au ions exhibits an extremely significant quenching effect on the luminescence intensity of TTB-COF in water, while other transition metal ions such as Fe^{3+}, Ni^{2+}, Co^{2+}, Zn^{2+}, and Cd^{2+} show relatively little photoluminescence quenching. Only a small amount of the investigated ions was adsorbed (Fig. 2f). In the mixture solution of Au^{3+}, Fe^{3+}, Ni^{2+}, Co^{2+}, Zn^{2+}, and Cd^{2+} ions at each concentration of 10 ppm, TTB-COF still retains high capture efficiency for Au ions (Inset in Fig. 2f).

An analogue of TTB-COF, COF-42 without thioether chain,[10] was used as the fluorescent probe for Au ions, however, only a weak response to Au ions was observed under the identical conditions (Fig. S20 and S21, ESI†). Only 14% Au ions can be captured by COF-42, which was far less than the adsorption effect of TTB-COF (Fig. 3a and Fig. S22, ESI†). This indicates that the fluorescence quenching and the Au ions capture ability of TTB-COF mainly result from the interactions between the sulfur groups in TTB-COF and Au ions, which was further verified by X-ray photoelectron spectroscopy (XPS). In comparison with XPS spectra of TTB-COF, the binding energy peaks of N 1s and O 1s in TTB-COF after Au capture (designated Au/TTB-COF) were still remained at 399.6 eV, 530.9 eV, and532.9 eV (Fig. S23 and S24, ESI†), respectively, whereas the binding energy of S $2p_{3/2}$ upshifted from 163.2 to 165.7 eV (Fig. 3b), indicating the specific and strong coordination interactions between S atoms and Au ions in Au/TTB-COF.[14] FTIR and XRD analyses of Au/TTB-COF revealed that no alternation in the crystalline and chemical structures were observed, reflecting the high structural stability of TTB-COF in Au recovery application (Fig. S25 and S26, ESI†). SEM images of Au/TTB-COF show the sheaf-like hierarchical microrods morphology is well remained (Fig. S27, ESI†). No obvious Au particles were observed in TEM images (Fig. S28, ESI†). Energy-dispersive spectroscopy (EDX) elemental mapping images of Au/TTB-COF demonstrate that the uniform distribution of the Au atoms within the framework is related to the location of S elements (Fig. 3c and 3d), which is in agreement with XPS results.

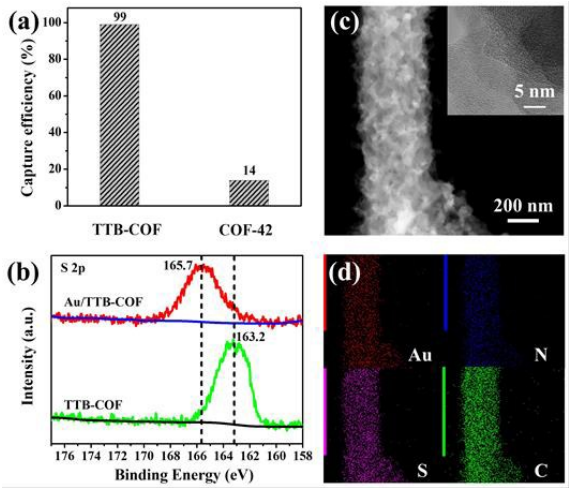

Fig. 3 (a) Comparison of Au capture efficiency of TTB-COF and COF-42 in aqueous solutions. (b) S 2p XPS spectra of TTB-COF and Au/TTB-COF. (c) TEM and (d) EDX elemental mapping images of Au/TTB-COF.

To enrich Au ion from water at the low concentration, Au/TTB-COF was treated with aqueous Na_2S solution. A gradual color change of was Au/TTB-COF observed from yellowish to brown (Fig. 4a), which can be taken as a sign of the reduction Au ions to nanoparticles (NPs).[15] The emergence of plasmon band at 590~675 nm in the UV-Vis DRS spectrum indicated the formation of Au NPs in TTB-COF (designated Au(0)/TTB-COF)

(Fig. 4b), which was confirmed through TEM analyses. TEM images of Au(0)/TTB-COF illustrate Au NPs were dispersed on the surface of TTB-COF (Fig. 4c). The Au 4f XPS spectrum of the Au/TTB-COF displays Au^{3+} (91.4 and 89.1 eV) and Au^{+} peaks (87.4 and 85.1 eV). No Au^{0} signals could be detected before the reduction. After in situ reduction with Na_2S, the typical XPS peaks of Au^{0} appear at 88.4 (Au $4f_{5/2}$) and 84.4 eV (Au $4f_{7/2}$) (Fig. 4d), respectively. Meanwhile, the intensities of Au^{3+} and Au^{+} peaks clearly decrease. The appearance of Au^{0} could be assigned to the interior Au atoms in Au nanoparticles in Au(0)/nanoparticles, while Au^{+} are attributed to the surface Au atoms of the nanoparticles. Therefore, the pendant thioether groups in TTB-COF not only provide strong Au-S interactions but also stabilize the Au nanoparticles ions in nanoparticles. XRD pattern for Au(0)/TTB-COF displayed characteristic peaks of metallic Au (Fig. S29, ESI†). Au(0)/TTB-COF was then subjected to the next Au ions capture run. Gratifyingly, the Au ions adsorption capacity was still up to 98% even after four cycles (Fig. 4e). Upon further pyrolysis to decompose the COF, high-purity metallic Au is obtained (metallic Au in Fig. 4a).

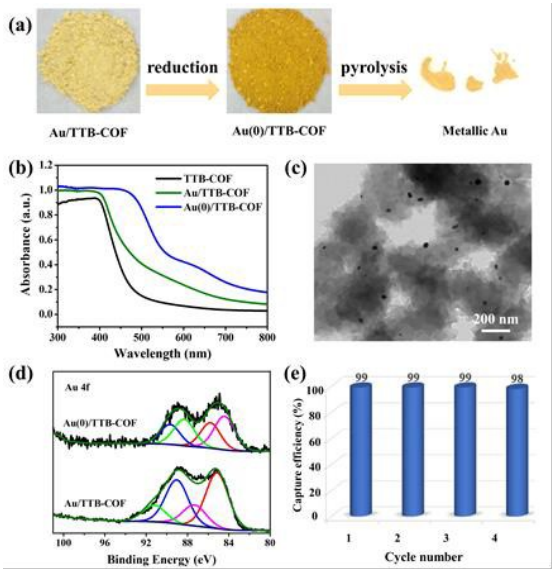

Fig. 4 (a) Photos of Au/TTB-COF, Au(0)/TTB-COF and Metallic Au. (b) UV-Vis absorption spectra of TTB-COF (black), Au/TTB-COF (green), and Au(0)/TTB-COF (blue) in the solid state. (c) TEM of Au(0)/TTB-COF. (d) Comparison of the Au 4f XPS spectra of Au(0)/TTB-COF and Au/TTB-COF. (e) Reuse studies of TTB-COF for Au ion capture in aqueous solution.

In conclusion, we have developed an effective COF with pendant thioether arms for selective sensing and recovery of Au ions in water. Significantly, given the specific coordination interactions between thioether groups and Au ions as well as the well-defined 2D conjugated COF structures, TTB-COF exhibits superb fluorescence sensing and capture efficiency in ultra-low concentration Au ions detection and recovery. Metallic Au powder with high purity can be obtained by further reduction and pyrolysis treatments. This work not only highlights the feasibility of sulfur-functionalized COFs for sensing and recovery of low concentration of Au ions in water but also stimulates further studies toward developing more functional COFs for novel applications through rational design at the atomic/molecular level.

We thank the National Natural Science Foundation of China (No. 51672046, 51672047, 51472050 and 21403238) and the Open Project Program of the State Key Laboratory of Photocatalysis on Energy and Environment (No. SKLPEE-KF201815).

Conflicts of interest

There are no conflicts to declare.

Notes and references

1 S. Syed, *Hydrometallurgy*, 2012, **115-116**, 30-51.
2 (a) Z. Liu, M. Frasconi, J. Lei, Z. J. Brown, Z. Zhu, D. Cao, J. Iehl, G. Liu, A. C. Fahrenbach, Y. Y. Botros, O. K. Farha, J. T. Hupp, C. A. Mirkin and J. Fraser Stoddart, *Nat. Commun.*, 2013, **4**, 1855; (b) C. Yue, H. Sun, W. Liu, B. Guan, X. Deng, X. Zhang and P. Yang, *Angew. Chem., Int. Ed.*, 2017, **56**, 9331-9335.
3 A. P. Cote, A. I. Benin, N. W. Ockwig, M. O'Keeffe, A. J. Matzger and O. M. Yaghi, *Science*, 2005, **310**, 1166-1170.
4 (a) N. Huang, P. Wang and D. Jiang, *Nat. Rev. Mater.*, 2016, **1**, 16068; (b) S. Ding and W. Wang, *Chem. Soc. Rev.*, 2013, **42**, 548-568. (c) H. Liao, H. Wang, H. Ding, X. Meng, H. Xu, B. Wang, X. Ai and C. Wang, J. Mater. Chem. A, 2016, **4**, 7416-7421.
5 (a) M. Zhu, S. Xu, X. Wang, Y. Chen, L. Dai and X. Zhao, *Chem. Commun.*, 2018, **54**, 2308-2311; (b) G. Lin, H. Ding, D. Yuan, B. Wang and C. Wang, *J. Am. Chem. Soc.*, 2016, **138**, 3302-3305; (c) S. Dalapati, E. Jin, M. Addicoat, T. Heine and D. Jiang, *J. Am. Chem. Soc.*, 2016, **138**, 5797-5800. (d) G. Lin, H. Ding, R. Chen, Z. Peng, B. Wang and C. Wang, J. Am. Chem. Soc., 2017, **139**, 8705-8709.
6 (a) Q. Gao, X. Li, G. Ning, K. Leng, B. Tian, C. Liu, W. Tang, H. Xu and K. P. Loh, *Chem. Commun.*, 2018, **54**, 2349-2352; (b) C. Zhang, S. Zhang, Y. Yan, F. Xia, A. Huang and Y. Xian, *ACS Appl. Mater. Interfaces*, 2017, **9**, 13415-13421; (c) W. Li, C. Yang and X. Yan, *Chem. Commun.*, 2017, **53**, 11469-11471; (d) S. Ding, M. Dong, Y. Wang, Y. Chen, H. Wang, C. Su and W. Wang, *J. Am. Chem. Soc.*, 2016, **138**, 3031-3037.
7 R. Xue, H. Guo, T. Wang, L. Gong, Y. Wang, J. Ai, D. Huang, H. Chen and W. Yang, *Anal. Methods* 2017, **9**, 3737-3750.
8 (a) Q. Yu and J. B. Fein, *Environ. Sci. Technol.*, 2017, **51**, 14360-14367; (b) C. Wang, L. Tian, W. Zhu, S. Wang, N. Gao, K. Zhou, X. Yin, W. Zhang, L. Zhao and G. Li, *Chem. Sci.*, 2018, **9**, 889-895.
9 L. Stegbauer, K. Schwinghammer and B. V. Lotsch, *Chem. Sci.*, 2014, **5**, 2789-2793.
10 F. J. Uribe-Romo, C. J. Doonan, H. Furukawa, K. Oisaki and O. M. Yaghi, *J. Am. Chem. Soc.*, 2011, **133**, 11478-11481.
11 Q. Sun, B. Aguila, J. Perman, L. D. Earl, C. W. Abney, Y. Cheng, H. Wei, N. Nguyen, L. Wojtas and S. Ma, *J. Am. Chem. Soc.*, 2017, **139**, 2786-2793.
12 (a) L. Li, L. Li, C. Cui, H. Fan and R. Wang, *ChemSusChem*, 2017, **10**, 4921-4926; (b) G. Gao, H. Wu, S. Ding, L. Liu and X. W. Lou, *Small*, 2015, **11**, 804-808.
13 (a) S. Bratskaya, Y. Privar, A. Ustinov, Y. Azarova and A. Pestov, *Ind. Eng. Chem. Res.*, 2016, **55**, 10377-10385; (b) C. Wu, X. Zhu, Z. Wang, J. Yang, Y. Li and J. Gu, *Ind. Eng. Chem. Res.*, 2017, **56**, 13975-13982; (c) K. Fujiwara, A. Ramesh, T. Maki, H. Hasegawa and K. Ueda, *J. Hazard. Mater.* , 2007, **146**, 39-50.
14 R. McCaffrey, H. Long, Y. Jin, A. Sanders, W. Park and W. Zhang, *J. Am. Chem. Soc.*, 2014, **136**, 1782-1785.
15 M. A. Huergo, L. Giovanetti, M. S. Moreno, C. M. Maier, F. G. Requejo, R. C. Salvarezza and C. Vericat, *Langmuir*, 2017, **33**, 6785-6793.

View Article Online
DOI: 10.1039/C8CC05369C

TOC

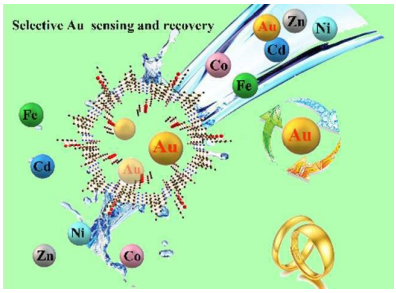

Ultra-low concentration of Au in aqueous solution is selectively detected and recovered by using a covalent organic framework bearing thioether pendant arms.